

Supporting Information

Molecular Relays in Nanometer Scale Alumina: Effective Encapsulation for Water-Submersed
Halide Perovskite Photocathodes

Yuval Harari,¹ Chandra Shakher Pathak,¹ Eran Edri^{1,2,3*};

¹Department of Chemical Engineering, Ben-Gurion University of the Negev, Be'er-Sheva 8410501, Israel

²Ilse Katz Institute for Nanoscale Science and Technology, Be'er-Sheva 8410501, Israel

³Blechner Center for Industrial Catalysis and Process Development, Be'er-Sheva 8410501, Israel

*To whom correspondence should be addressed

SI-1. Physical characterization of CsPbBr₃ and CsPbBr₃ solar cell.

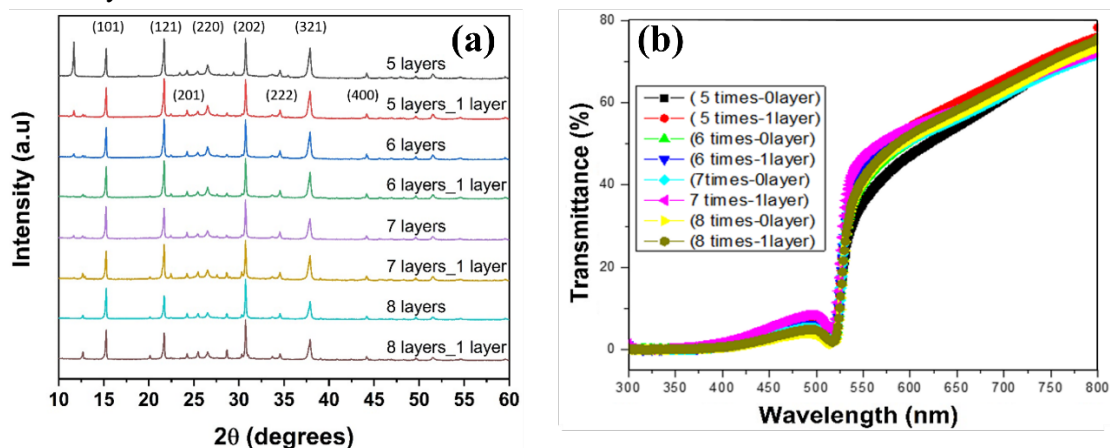


Figure S1. X-ray diffractogram and transmittance spectra of CsPbBr₃ films. The number of applied PbBr₂ and CsBr coatings are shown in the figure (x layers/times – y layers represent the number of PbBr₃ and CsBr coating cycles applied).

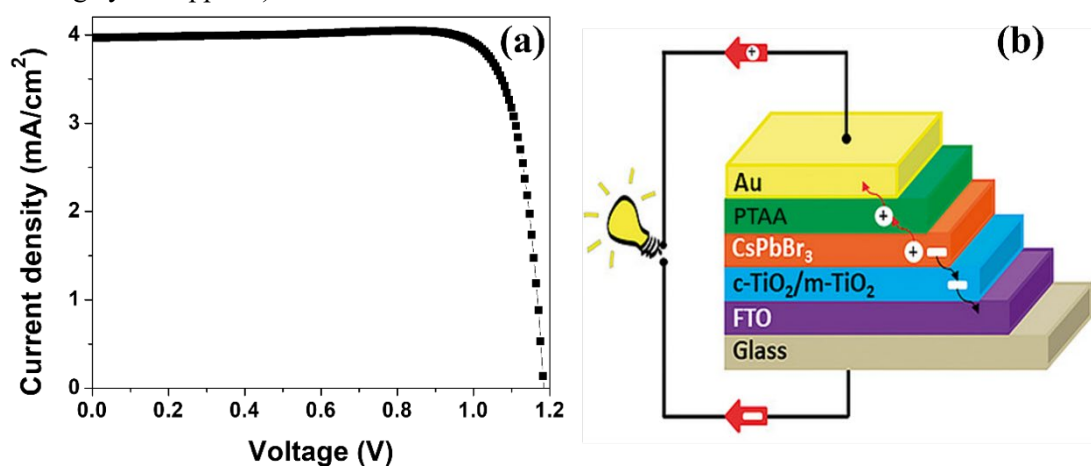


Figure S2. (A) the current-voltage curve of CsPbBr₃-based solar cell. (B) An illustration of the solar cells' layered structure.

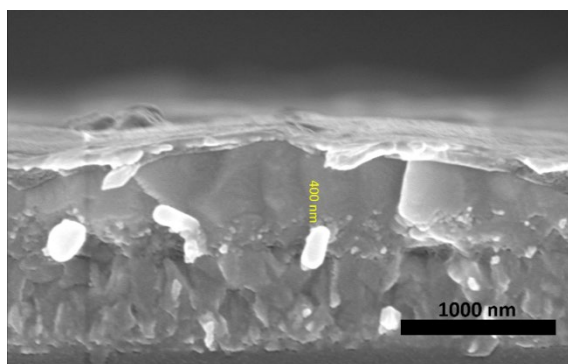


Figure S3. Cross-section SEM image of the CsPbBr₃ solar cell.

SI-2. Compact NiOx.

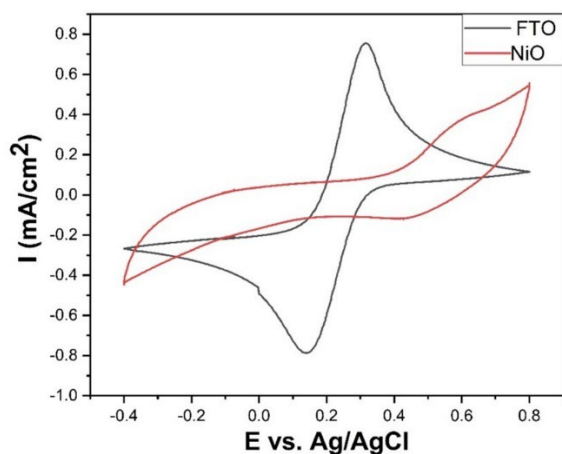


Figure S4. Cyclic voltammogram of NiO/FTO and FTO. Using FTO (red) and NiO/FTO (blue) electrodes as a working electrodes for redox reaction of $K_3Fe(CN)_6$ in aqueous solution. Ag/AgCl was used as the reference electrode and a Pt rod as the counter electrode. In the case of FTO, the electrode presents oxidation and reduction peaks, while NiO/FTO presents only an oxidation reaction peak.

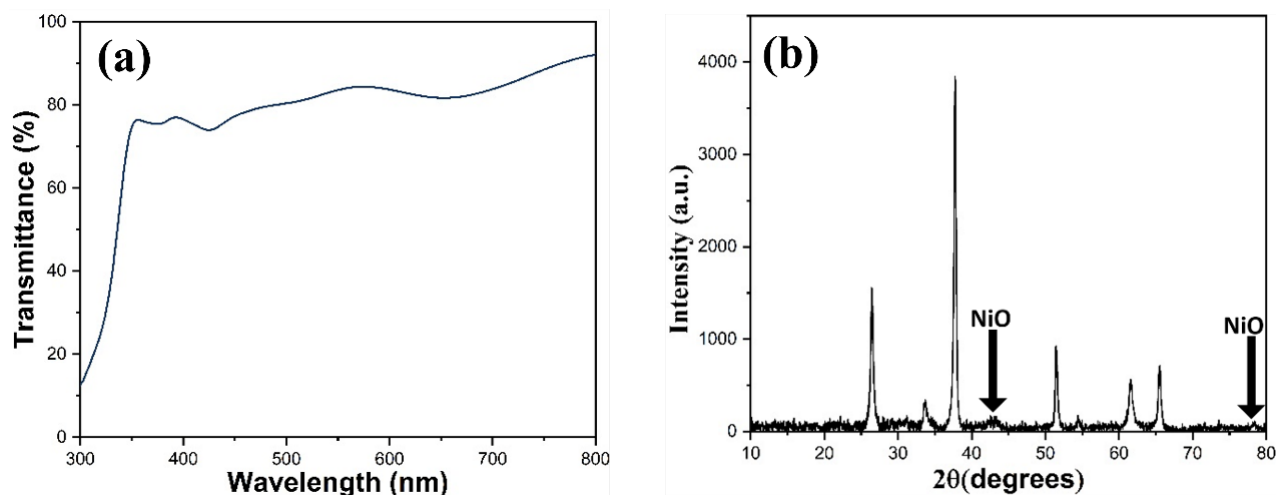


Figure S5. (a) UV-Vis Transmittance spectrum of NiO/FTO. The transmittance band at ~ 350 nm relates to absorption. (b) XRD spectrum of NiO/FTO. The peaks related to NiO are marked, and the other relates to the FTO substrate. The FTO peaks overshadow NiO peaks at $\sim 37^\circ$ and $\sim 62^\circ$, which were small and merged with the FTO peaks.

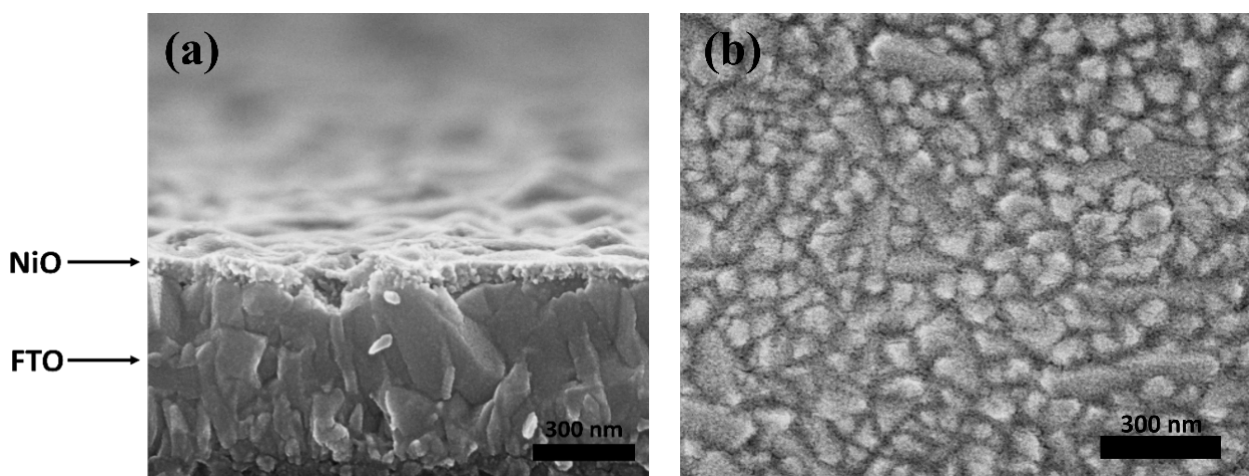


Figure S6. SEM images of compact NiO on FTO substrate. (a) Cross-sectional SEM image; X50,000 magnification. Arrows mark the FTO substrate and the NiO film. Can distinguish between the two different morphologies. (b) Top view of the NiO/FTO sample.

SI-3. Protective layers

Table S1. CsPbBr₃ stability measurement in different combinations of protective layers.

<i>Al₂O₃ thickness (nm)</i>	<i>TiO₂ thickness (nm)</i>	<i>Stable (V)</i>	<i>Unstable (X)</i>
0	10	X	
0	30	X	
0	70	X	
4	0	X	
6	0	X	
8	0	X	
10	0	V	
4	10	X	
4	30	X	
4	70	V	

SI-4. Molecular attachment.

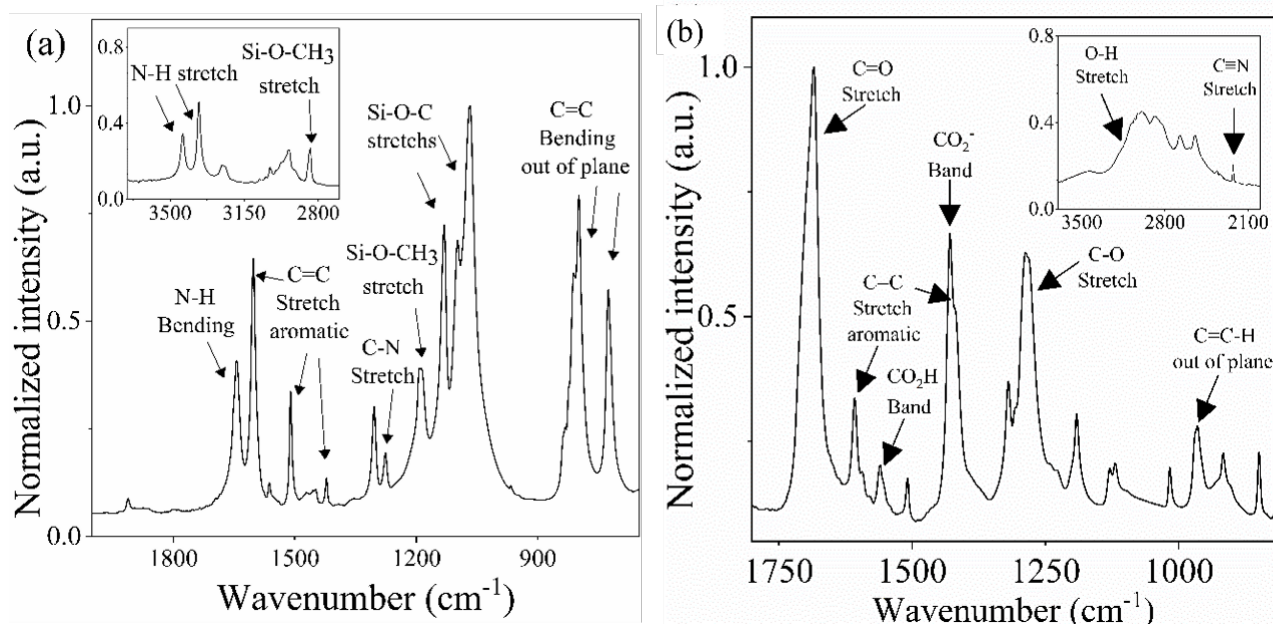


Figure S7. FTIR spectra of TMSA and CMs in a KBr pellet. (a) FTIR spectrum of the linker molecule – TMSA. The peaks of the functional groups from the molecules are indicated. (b) FTIR spectrum of the CMs in KBr pellet. The spectra were measured in transmission; 100 scans with a resolution of 4 cm⁻¹ were averaged.

SI-5. cp-AFM

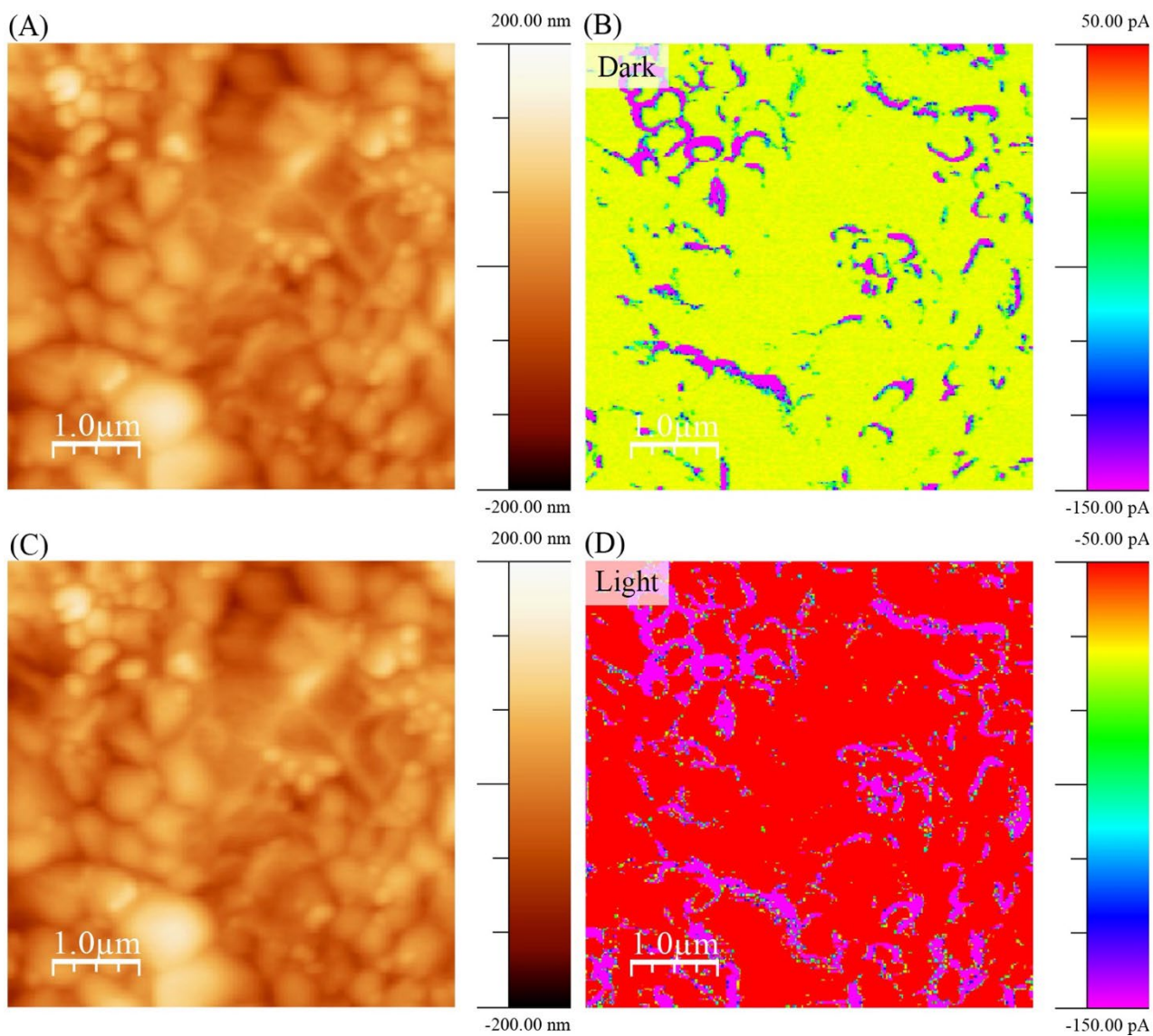


Figure S8. Conductive probe AFM scans of CsPbBr₃/NiO electrodes (without CMs) under light and bias. (A) and (C) topography scans. (B) Current map in the dark. (D) Current map in the light.

SI-5. The functionality of CMs.

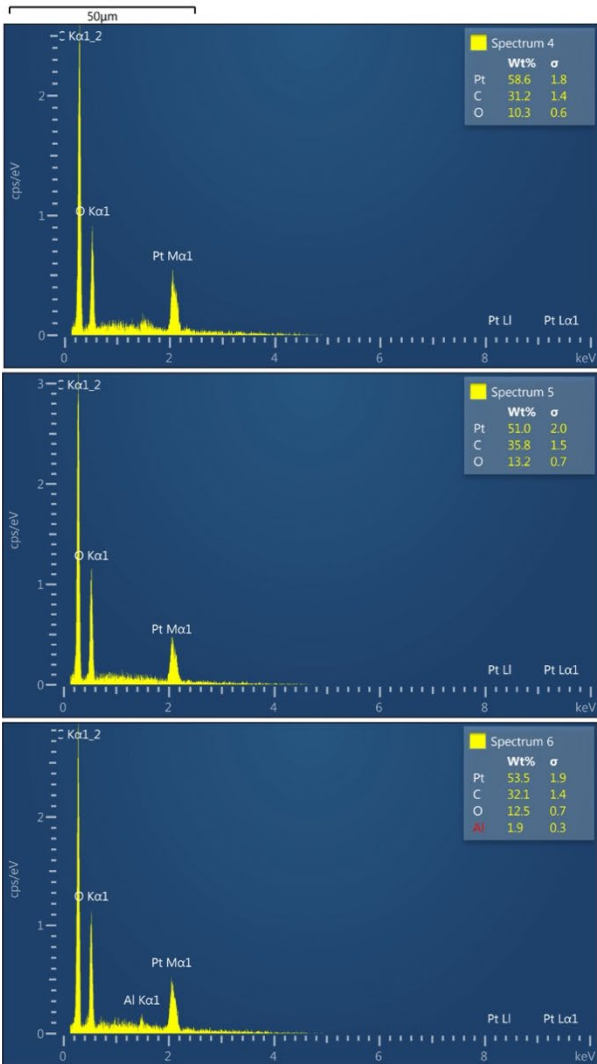
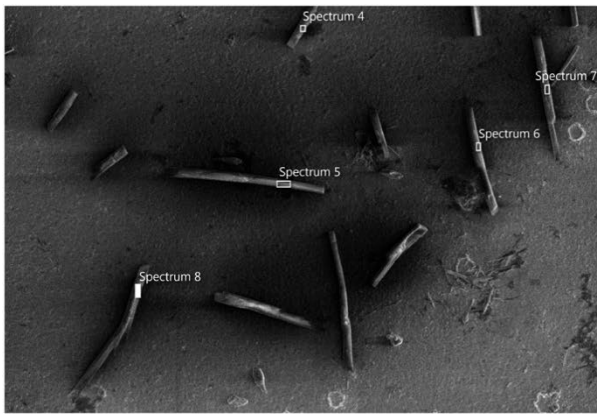


Figure S10. SEM image and EDS of Pt rods. The EDS spectra were collected from the regions designated in the SEM image.

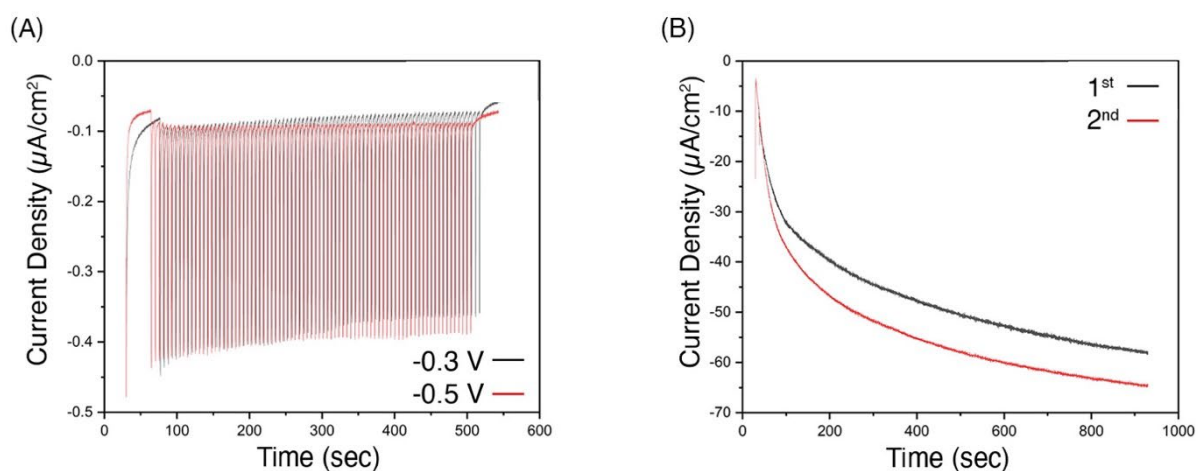


Figure S11. Chronoamperometry of Pt and Ag photo-electrodeposition on CsPbBr₃. (A) Chronoamperograms of Pt photo-electrodeposition with a bias voltage of -0.3 and -0.5 V (vs. Ag wire). (B) Chronoamperograms of two sequential photo-electrodepositions of Ag with a bias voltage of -0.9 V (vs. Ag wire). The first deposition cycle (black trace) showed an overall lower photocurrent than the second deposition cycle (red trace).

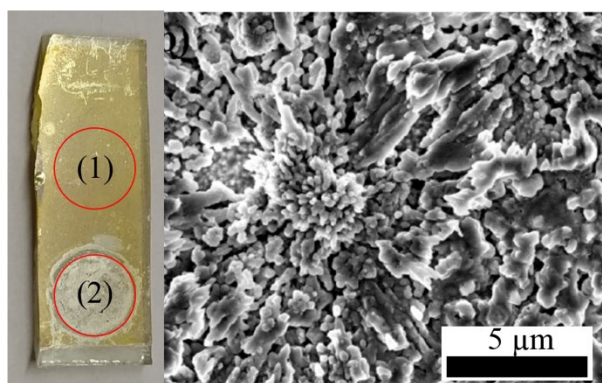


Figure S12. A picture of an Ag/CMS-alumina/titania/HaP/NiO/FTO. Region (1) is an area that was exposed to the electrolyte for ~1 hr. Region (2) is a region that was exposed to electrolyte and bias potential for several minutes. The SEM image is taken from the region (2). Ag was photo-electrodeposited.